Advances in Bioresearch
Adv. Biores., Vol 12 (1) January 2021: 102-117
©2021 Society of Education, India
Print ISSN 0976-4585; Online ISSN 2277-1573
Journal's URL:http://www.soeagra.com/abr.html
CODEN: ABRDC3
DOI: 10.15515/abr.0976-4585.12.1.102117

Advances in Bioresearch

ORIGINAL ARTICLE

Callus mediated biosynthesis of Zinc oxide nanoparticles using *Catharanthus roseus* grown under various physiological conditions & their characterization: A novel approach to develop potent antimicrobial drug

Monika Gupta[1*]
[1]Amity Institute of Biotechnology, Amity University Madhya Pradesh, Maharajpura road, Gwalior (MP)-474005, India
*Corresponding author email: biotech.monikaphd@gmail.com

ABSTRACT
The current research work is an attempt to develop a common laboratory procedure for synthesis of nanoparticles from C. roseus under controlled conditions. C. roseus, an important medicinal plant, has numerous secondary metabolites which act as reducing and capping agents through which size of nanoparticles can be regulated. Regulating size and morphology of nanoparticles under in-vitro conditions has been less focused and challenging. The present work also focuses to develop greener, highly feasible, rapid and cost-efficient methods to produce nanoparticles. The callus culture was exposed to altering photoperiods (16/8 hours light and dark: controlled, 16/8 hours dark/light: short days, 20/4 hours light/dark: long days). In another experiment, pH was also changed and callus was maintained at pH 5.0, 6.5, 7.0 under control light conditions. The callus was collected to reduce ZnO and form ZnO NPs. It was found that the best callus with optimum pigmentations was formed at pH 5.7 and under control light conditions. ZnO NPs synthesized from this callus demonstrated highest antibacterial activity against six different microbes. Moreover, these ZnO NPs were thoroughly characterized using various techniques viz. UV-Visible analysis, FTIR, XRD, SEM, TEM, EDX, AFM and DLS to determine morphology, size, presence of functional groups and dispersity. This research work provides the most recent and innovative technique for the development of nanoparticles through callus under controlled conditions thereby producing accurate-sized nanoparticles which increases their antimicrobial potency significantly.
Keywords: *Physiological conditions; Callus; characterization; monodispersity; antimicrobial efficacy.*

Received 11.11.2020 Revised 26.12.2020 Accepted 21.01.2021

How to cite this article:
Monika Gupta. Callus mediated biosynthesis of Zinc oxide nanoparticles using *Catharanthus roseus* grown under various physiological conditions & their characterization: A novel approach to develop potent antimicrobial drug. Adv. Biores., Vol 12 (1) January 2021: 102-117

INTRODUCTION

ZnO NPs have gained attention in various fields like photo catalysis, piezoelectric film, solar cells, biosensors, water purification [1, 2]. ZnO NPs are also used in cosmetics and many biomedical fields as they UV radiation [3]. For the synthesis of ZnO NPs, several methods are available viz. ion implantation, chemical vapour deposition [4], sol-gel process [5] in various literatures. Most of these methods use hazardous reducing agents and organic solvents. To minimize this, the relatively new and largely unexplored bio-inspired approach of synthesis were developed and employed which can be rapid, cheaper, reliable and high yielding process.

Identifying a plant which is rich in bioactive compounds is a pre-requisite. *C. roseus* is one such medicinal plant which contains many metabolites namely Terpenoids-indole alkaloids (TIA): Catharanthine Vincristine, Serpentine, Ajmalicine and Vinblastine. In this current research, callus extract route was chosen to synthesize ZnO NPs from *in-vitro* grown *C. roseus* under controlled conditions. The metabolites act as reducing and capping agents during reaction.

Before synthesizing nanoparticles, callus extract was tested in two separate experiments: changing amount of light keeping pH constant (5.7) and changing pH keeping light constant (16 h light & 8 h dark). This gives flexibility to regulate size and morphology of nanoparticles as nanoparticles with uniform size and morphology and controlled structure has many biomedical applications. Monodispersity in nanoparticles, which had been a challenge since long time, has been achieved in this study.
To determine and confirm all these parameters: size, morphology, presence of functional groups, dispersity and metal percentage, various characterization techniques have been employed viz. UV-Vis spectroscopy, SEM, TEM, XRD, DLS, FTIR and AFM. Post characterization, these nanoparticles with regulated features are ready for antibacterial action.
ZnO NPs are very small sized and have a large surface to volume ratio which makes them capable to enter bacterial cell wall and rupture it which eventually leads to cell death (6). Thus they prove better than existing antibiotics by combating multi-drug resistant bacteria. They have also been used as an anticarcinogenic agent against various cancer cells. This study further tests the antibacterial efficacy of ZnO NPs against 6 pathogens by 2 methods: Disk diffusion & MIC. The **a**im of this study was used to grow callus of *Catharanthus roseus* by plant tissue culture method. In this process, callus was subjected to light and pH alterations aimed to develop monodispersed nanoparticles with high antibacterial efficacy.

MATERIAL AND METHODS

For the formation of callus culture, leaf explants were taken from the *in vitro* grown plantlets of *C. roseus* and inoculated on MS media.

Sample preparation

Cultivars of *C. roseus* seeds were procured from the local nursery of Gwalior, India. The seeds were then surface sterilized and treated with 0.1 % $HgCl_2$ for 1-2 min and kept for 4 -5 weeks under in-vitro conditions.

Media preparation for induction of callus

MS medium was prepared for in-vitro cultivation of seed and pH of the medium was adjusted to 5.7. After this the solution was autoclaved at 121 °C and pressure at 15 pounds/inch for twenty minutes and filter sterilized PGRs were added into the MS medium.

Surface Leaf sterilization

Surface leaf sterilization of leaf explants was done by treating with 1% Tween 20 for 15 minutes and washing with 70% ethanol for 5-10 minutes. Consequently, the explants were surface sterilized with 0.1% $HgCl_2$ and further with autoclaved water [7].

2.2.2 Callus germination

Further, leaf explants were cut into very small parts (in mm). These tiny parts were transferred into MS media containing variable levels of auxins and cytokinins (BAP 3mg/ml + NAA 1mg/ml). After three weeks of incubation, friable greenish and nodular calli appeared (8).

$$\text{Callus Induction Frequency} = \frac{\text{No. of explants showing response}}{\text{Total No. of explants inoculated}} \times 100$$

Frequency = No. of explants showing response /Total No. of explants inoculated×100

The effect of different photoperiods and pH on callus was observed and the best callus was collected for the biosynthesis of NPs.

Biosynthesis of ZnO NPs from callus extract

After surface sterilization of callus, it was then dried in dark at 25°C and ground into fine powder. The dried powder (10 gm) was dissolved in 100 ml of sterilized water and kept overnight (9). The extract was filtered and the filtered extract was centrifuged at 3000 rpm for 20 min at 25°C. The transparent part which floats above is collected to synthesize ZnO NPs.
Biosynthesis of ZnO NPs was performed by mixing the 50 ml of an aqueous solution of 0.01M zinc acetate dehydrate with 1 ml callus extract separately and followed by constant stirring till the formation of the white suspension (10). The pH was adjusted to 12.0 using 2M NaOH and kept on stirring until the ZnO NPs precipitate was completely dissolved. The spectra exhibited an absorption band with a resolution of 1.0 nm between 350 and 500 nm (11); this indicated the formation of ZnO NPs.

Characterization techniques for ZnO NPs

Different physicochemical features of nanoparticles are determined using multiple characterization techniques (12).

UV-Vis spectra analysis

The absorbance of the ZnO NPs was obtained using a double beam UV-Visible spectrophotometer (Model-Shimadzu UV- 2450, Japan) in the range of 300 - 600 nm.

 © 2021 Society of Education, India

XRD analysis

An X-ray diffract meter operated at 40 kV and 30 mA and at 2θ angle pattern with scanning range of 20^0 - 80^0 (Model- Rigaku- miniFlex600) is used and their size is determined by the Debye-Scherrer equation $\mathbf{D = 0.9\,\lambda / \beta \cos\theta}$

FTIR analysis

The dried powder sample was prepared by mixing purified nanoparticles with 10 mg of potassium bromide powder, and then dried to remove the moisture content, after which the FTIR characterization was performed using Perkin- Elmer FTIR-105627, USA to determine various functional groups and secondary metabolites present on the surface of nanoparticles that act as reducing and capping agents.

DLS analysis

500 µl of nanoparticles solution diluted with 3 ml of sterilized distilled water was poured into the zeta dip cell and measured by intensity vs time graph which gives the polydispersity index (size distribution profile) of ZnO NPs. (Instrument : nano plus - Zetasizer).

AFM analysis

A thin film of the colloidal solution of silver nanoparticles was prepared on a glass substrate by placing few drops of the solution on the glass substrate and dried for 15 min. The thin film on the glass substrate was scanned with the AFM (NT-MDT, Russia) which gave 3-D imaging and surface topology of the synthesized ZnO NPs.

SEM , TEM and EDX analysis

Few drops of colloidal solution of ZnO NPs were put on a carbon-coated copper grid substrate and dried under a mercury lamp. The samples were then characterized using SEM, TEM and EDX, JEOL Model-LV6490 which gave size, morphology and elemental composition.

Anti bacterial activity of ZnO NPs

Disc Diffusion Method

The antibacterial potential of ZnO NPs was determined against six different pathogenic bacteria (*S. aureus* MTCC 9760, *S. pyogenes* MTCC1926*, B. cereus* MTCC 430, *P. aeruginosa* MTCC 424, *P. mirabilis* MTCC 3310 *and E. coli* MTCC 40), by the standard disk diffusion method (13, 14). Whatman filter paper no.1 disks consisting of 500, 700, 1500 µg/ml of ZnO NPs combined with 10µg/ml streptomycin per disk were used for the assay. MHA was used to grow bacteria. The overnight grown cultures of tested bacteria were serially diluted to 1×10^{-7} CFU were used for the assay. The antibacterial activity was determined by measuring the diameter of zones of inhibition around the filter paper disks after 24h of incubation at 37^oC.

MIC Method

MIC was determined against the serially diluted bacterial concentration of 10^{-5}, 10^{-6}, 10^{-7} CFU/ml along with different concentrations of ZnO NPs (15). These serially diluted bacterial concentrations were prepared by mixing 9ml MHB and 1 ml of 10^{-5}, 10^{-6}, 10^{-7} bacterial concentrations serially and then incubated for 24 hrs. and at 37°C. The growth curve of bacteria (Gram +ve and Gram –ve) is examined by measuring optical density (OD) taken at 590 nm (15).

RESULT AND DISCUSSION

Effects of different physio-chemical parameters: photoperiods and pH on callus growth

Light is a very important physical factor for callus growth and development illustrated in (Figure 2). It was observed, under controlled light conditions (16 hrs light and /8 hrs dark), photosynthetic mechanism is carried out by the cells of induced calli, and they produce pigments which make them autotrophic in nature. Carbohydrates, proteins and other primary and secondary metabolites are produced by these cells of induced calli under both conditions (light and dark). Concerning the callus morphology, callus grown under light condition were relatively compact as compared to that grown under dark condition (Figure 1). Significant differences were observed in the development of greenish calli in contact with different lighting conditions (Figure 1). Callus growth was observed under the control condition followed by SD (8 h light/16 h dark) and LD (20h light/4 h dark) until 7 to 14 days. The callus growth was fast, compact and appeared greenish at control condition with pH 5.7 medium as compared to other growth conditions (pH 5.0, pH 6.5 and pH 7.0). The callus growth was inhibited at SD and LD, indicating that minimum and excess exposure to light can inhibit callus growth. Under the controlled light condition, the fresh weight of callus was twice as compared to callus incubated at LD. Moreover, fresh weight of callus grown in dark was much lesser as compared to callus developed under controlled condition. This report indicates that the lack of light was not favorable for the growth and development of callus. Changes in callus pigments were also observed due to different light conditions, as seen in (Figure 1). Under control condition, after 7 days of treatment, callus showed greater survival and was greenish in colour due to

favorable conditions. Similar results were also observed after 14 days of treatment. Under SD condition, callus appeared brown and yellow due to the accumulation of phenols after 7 days. As increase the treatment for 14 days, callus appeared in decline phase due to the turn down of photosynthesis reaction. Under LD condition, the appearance of callus turn into brown colour within 1 week, and after 14 days, it converted into brownish to black colour (Figure 1). These results suggested that during SD and LD, phenolics levels increase considerably which gives brown to black colour to the callus. Our results are in close agreement with the work published by Kami *et al*. (16). They demonstrated the effect of light and dark conditions on callus induction and growth.

Characterization of ZnO NPs from callus formed under different photoperiods and different pH (5.0, 6.5, 7.0)

UV Spectroscopy Analysis

The formation of ZnO NPs was confirmed by the colour change of nanoparticles suspension from colorless to white pale colour (17). This is also indicated by well-defined SPR band at around 367 nm for CME-ZnO NPs at 7days (control), 360 nm for CME-ZnO NPs at 14 days (control) at pH 5.7 (Figure 2; A).

In case of 7 &14 days SD, the absorption peak was obtained at 373 nm and 378 nm (Figure 2; B). In 7 & 14 days LD, the absorption peak was obtained at 377 nm and 373 nm corresponding to transverse SPR component of triangular and spherical ZnO NPs. The SPR band should remain between 350- 378 nm for ZnO reaction (17). The shift in SPR peak indicates a change in the size of ZnO NPs, and hence, any shift of the peak toward the longer wavelength is accompanied by the large size of ZnO NPs (Figure 2; A & B).

The main effect of reaction pH is the ability to change the electricity charges of biomolecules, which can reduce their capping ability and subsequently their shape and size. Hence, ZnO NPs were synthesized by CME at different pH: pH 5.0, 6.5, 7.0. The formation of nanoparticles was confirmed by the colour change in CME suspension from transparent yellowish into pale white. The formation of ZnO NPs was reconfirmed by UV-Visible spectra analysis (Figure 2; C) in which broad peaks were observed at 375 nm for pH 5.0, 377 nm for pH 6.5, and 460 nm for pH 7 (Figure 2; C). When the pH of solution increases from pH 5 to 7, the absorption peak intensity got shifted. The broadening of the SPR peak indicates the existence of a wider range of sizes in the solution which makes them unfit for antimicrobial activity.

XRD analysis

Figure 3:A indicates that ZnO NPs from CME-7 days (control) and at pH 5.7 show the characteristic peaks corresponding to (100), (002), (101), (102), (110), (103), (201) and (202) of ZnO are located at 2θ of 31.880, 34.520, 36.340, 47.660, 56.680, 62.940, 68.040 and 77.020 respectively. While for ZnO NPs from CME-14 days (control), it showed a peak at 31.980, 34.60, 36.480, 47.720, 56.840, 62.940, 68.160, 77.080 and 81.50, corresponding to the same (hkl) Bragg reflection peak like that for 7 days (control). Figure 3: A & B shows XRD peaks of ZnO NPs synthesized using CME-7 & 14 days SD and CME-7 & 14 days LD. These Bragg's reflection peaks denotes that the crystalline phase of ZnO NPs matches with JCPDS card no.79-0207 for ZnO NPs. Similarly, all the results of the highest intensity peaks were found at 36.340 assigned to (101) and (002). The result indicates that the sample is composed of a hexagonal wurtzite structure. Broadening peak and noise were probably related to the presence of various crystalline biological molecules in the callus extracts. The sharp peaks indicate some bio-organic compounds present in the nanoparticles during the synthesis. The average crystallite size of ZnO NPs was calculated from the XRD outline according to the line width of the (1 0 1) peak through the "Debye-Scherrer equation". The average particle size of the ZnO NPs using 7 & 14 days control CME was around 18.17 and 18.38 nm. For 7 & 14 days SD-CME synthesized ZnO NPs average size was around 18.18 nm & 20.09 nm. For 7 & 14 days LD-CME synthesized ZnO NPs average size was around 25.40 nm & 18 nm respectively. The smallest sized nanoparticles were found to be in Control-CME based ZnO NPs.

Figure 3: C represents the XRD pattern of the ZnO NPs synthesized by CME at pH 5.0, 6.5 and 7.0. The diffraction peaks data found were in accordance with the reports of FCC structure from (JCPDS) file No. 79-0207. During the formation of nanoparticles, impurities were obtained for all the pH 5.0, 6.5, 7.0 which are marked by (*) (Figure 3: C). Hence the best pH for callus mediated synthesis of ZnO NPs was pH 5.7 and under controlled light conditions.

FTIR analysis

To examine the functional groups attached to the surface of ZnO NPs, FTIR spectra analysis was used. In figure 4: A, ZnO NPs formed by CME-7 days (Control) and at pH 5.7 showed peaks at around 3437, 1634, 1486, 1425, 1384,1020, 885, 666 and 551 cm^{-1} which correspond to the groups (O-H) stretch, (C=C) stretch, (C-F) stretch, (C-H) bent and (C-Cl) stretch. Whereas for CME-14 days (Control) ZnO NPs peaks at around 3392, 1634, 1485, 1383, 886, 562, 535 and 518 cm^{-1} were obtained. Figure 4: A & B displays the FTIR peaks for synthesized ZnO NPs using CME-7 & 14 days (SD) and CME-7 & 14 days (LD). The Spectra of FTIR indicated that the reducing and stabilization of ZnO NPs by the coordination with O-H, C=O, C-I, C-

Br. These bands indicated the presence of terpenoids group in callus extract (18). It can be inferred that terpenoids, alcohols, carboxylic, ketones and aldehydes groups are present in synthesized nanoparticles which prevent agglomeration and provide them stability. Phenol compound, flavonoids, alkaloids and tannins were also present in callus for capping of the nanoparticles (19).

The FTIR measurements of synthesized ZnO NPs by using CME for pH 5.0, pH 6.5 and pH 7.0 did not give proper peaks (Figure 4: C) because secondary structure of proteins remained unaffected during the reaction of metal salt of Zn ion into ZnO NPs.

EDX

The EDX analysis displays a strong indication in the zinc oxide region symbolizing the reduction of zinc oxide ion and hence the formation of ZnO NPs (Figure 5). The elemental composition for ZnO NPs formed by CME-7 days treated (Control) and at pH 5.7 was (23.16 %) Oxygen and (76.84%) Zinc whereas for CME-14 days (control) the elemental composition was (20.73%) Oxygen and (79.27%) Zinc (Figure 5: A1 & B1). These outcomes show the achievement of spherical sizes with uniform agglomeration. In case of ZnO NPs formed by CME-7 & 14 days (SD) and CME-7 & 14 days (LD), the percentage of Zinc in synthesized ZnO NPs dropped due to different light treatment on callus development (Figure 5: A2-A3 & B2-B3). The absorption peak of ZnO NPs was studied at 3 keV, which is a typical absorption of metallic ZnO NPs.

EDX study was done for the ZnO NPs formed by callus treated under different pH and control light conditions. At pH 5.0, pH 6.5, pH 7.0 the amount of Zinc was found to be on lower side : 54.65% , 59.23% and 57.09% respectively (Figure 5: C1-C3). Lower the amount of Zinc less effective would be the synthesized ZnO NPs.

DLS analysis

The size distribution, polydispersity index (PDI) and the average size of the particles of the green synthesized ZnO NPs were determined by DLS (Figure 6). The average particle size of ZnO NPs formed by CME-7 days (control) and CME-14 days (control) and at pH 5.7 was found to be 42.98 nm and 43.99 nm (Figure 6: A1 & B1). The Polydispersity index was 0.6 and 0.15 respectively which indicates that the synthesized nanoparticles are monodispersed. In case of ZnO NPs formed by CME-7 & 14 days (SD), the size was found 150 nm and 126 nm respectively and polydispersity index was found to be 1.0. For ZnO NPs by CME-7 & 14 days (LD), sizes were much larger: 213 nm and 239 nm respectively (Figure 6: A2 & B2 & A3-B3).

Polydispersity index > 0.7 indicates polydispersed nanoparticles. These results verify the presence of phytochemicals compounds in control light treated callus extract which had prevented the agglomeration of nanoparticles and produced monodispersed nanoparticles.

ZnO NPs formed by CME treated under different pH & control light conditions was again analyzed by DLS technique. At pH 5.7, the smallest particles of 48.98 nm and 98.99nm from control-CME at 7 & 14 days respectively were obtained (Figure 6). At pH 5.0, pH 6.5, pH 7.0 nanoparticles of size 530 nm, 633 nm and 820 nm respectively (Figure 6: C1-C3). Hence, pH 5.7 & control light conditions gave the smallest nanoparticles (42.98 nm and 43.99 nm). Smaller nanoparticles have higher antimicrobial efficacy.

AFM analysis

AFM is a biophysical technique for studying the morphology of nanoparticles and biomolecules. The 3D structure and the height of the ZnO NPs were investigated with AFM, and it indicates that the nanoparticles are needle-like in shape. For ZnO NPs formed by CME-7 days (control) and at pH 5.7, the height was in the range **30-40 nm**. Their topography showed uniformly dispersed and well scattered nanoparticles (Figure 7: A). For ZnO NPs formed by CME-7 days (SD) & 7 days (LD), the size increased to 120-150 nm and 200-250nm respectively (Figure 7: B & C). In the case of SD & LD, the AFM image revealed the large symmetric size of particles. These particles show strong agglomeration and a rough line profile. ZnO NPs thus show heterogeneous size and polydispersity in this case.

Size of nanoparticles were found to be approximately same for 14 days to that of 7 days when observed under other characterization techniques, hence analysis for 14 days was not considered in this technique.

The ZnO NPs extracted from CME treated under different pH were also analysed by AFM. . The AFM images of the ZnO NPs in 2D and 3D forms and height distribution is shown in (Figure 7: D-F). ZnO NPs formed by CME treated with pH 5.0, pH 6.5 and pH 7.0, the average diameter was found to be 100-120 nm, 150-200nm, 130-150nm respectively. Size has increased considerably due to change in pH of reaction media.

TEM analysis

TEM micrographs demonstrate that particles are hexagonal, uniformly distributed without any significant aggregation (Figure 8). The particles size histogram of synthesized ZnO NPs from CME-7 days (control) demonstrates that particles size ranges from 50 to 100 nm (Figure 8: A1 – A4). For ZnO NPs from CME-7

days (SD) particles size ranges from 160 to 240 nm with an average size of 197.68 nm Figure 8: B1-B4). The particles were spherical and hexagonal, but were polydispersed with agglomeration. For ZnO NPs from CME-7 days (LD) most nanoparticles showed sticky nature and the particles size ranges from 90 to 210 nm with an average size of 141.63 nm (Figure 8: C1-C3). Hence, only for 7 days control, ZnO NPs was found to be monodispersed, uniform and small sized.

The SAED patterns of ZnO NPs further suggest the crystalline nature of NPs which have already matched the results of XRD analysis. Particles size observed under TEM study is also close to that of the XRD analysis. The intermittent bright dots arranged in concentric Debye-Sherrer rings as (100), (002), (101), (102), (110), (103),(201) and (202) can be indexed to the same peaks of XRD for all of the synthesized ZnO NPs using CME-7 days Control, SD and LD (Figure 8: A3, B3 & C3). The results of the average particle size and distribution procured from TEM analysis matches well with DLS analysis by applying the histogram data with a Gaussian distribution. It has been observed that NPs of small sizes have been recorded in monodispersed form.

Antimicrobial activity of zinc oxide nanoparticles and synergistic activity

Disk diffusion method by Zone of Inhibition

ZnO NPs undergo a contact with the bacterial cell wall and show an effective antibacterial activity against Gram (+)ve and Gram (-)ve bacteria. When taken alone at concentration of 900µg/ml ZnO NPs formed from CME-7 days (control) and at pH 5.7 showed moderate antibacterial activity against six pathogenic bacteria indicated by diameter of ZOI (12.18 to 13.01 mm ZOI) while ZnO NPs formed from CME-14 days (control) at 900µg/ml alone had a ZOI of 12.78 – 13.10 mm (Table 1). It was also observed that ZnO NPs were more active against Bacillus cereus 430 MTCC {a Gram (+)ve bacteria} than Proteus mirabilis 3310 MTCC {a Gram (-)ve bacteria} both in case of 7 & 14 days (control).

The standard antibiotic, alone streptomycin at 10µg/ml did not show significant activity against the tested pathogens.

Hence, the 6 pathogens were tested for ZnO NPs in synergy with streptomycin. ZnO NPs formed from CME-7 & 14 days (control) displayed strong antibacterial activity against all the tested pathogens at 1500 µg/ml, with a ZOI ranging in diameter from 16.98 to 20.78 mm and 17.08 to 21.78 mm respectively (Table 1 and Figure 9: A). The maximum zones of inhibition were obtained at Gram (+)ve bacteria (S. aureus 9760 MTCC, S. pyogenes 1926 MTCC, B. cereus 430 MTCC) at 1500µg/ml concentration as compared to Gram (-)ve bacteria (P. aeruginosa 424 MTCC, E. coli 40 MTCC, P. mirabilis 3310 MTCC).

ZnO NPs synthesized from CME-7 & 14 days (SD) showed little antimicrobial activity against only 3 of the 6 bacteria (alone & with streptomycin). While for ZnO NPs formed from CME-7 & 14 days (LD) did not show any antimicrobial activity against any of the 6 bacteria (alone & with streptomycin). Results were similar for SD & LD at 1500µg/ml concentration also (Table 2: A & B and Figure 9: B & C).

ZnO NPs formed from callus treated at different pH 5.0, 6.5 and 7.0 were also tested for antimicrobial action but neither of them showed zone of inhibition against any of the 6 tested pathogens for all the pH (Table 3).

Antimicrobial activity by MIC Method

Figure 10 shows the MIC values of 1500µg/ml ZnO NPs as calculated by (OD) optical density at 590 nm wavelength. Higher concentrations of ZnO NPs (Figure 10: A-C) were found to completely inhibit bacterial growth than lower concentrations. Finally, for CME-ZnO NPs, the average MIC values were 1500µg/ml for both Gram (+)ve bacteria and Gram (-)ve bacteria . However, bactericidal activity of ZnO NPs formed using CME-7 & 14 days (control) was higher in Gram (+) ve bacteria as compared to Gram (-) ve bacteria (Figure 10: A).

This is due to the fact that the cell wall of the Gram (+) ve bacteria binds the metals in large quantities as compared to the Gram (-) ve bacteria (20). Small-sized ZnO NPs are more bactericidal than the larger ones (21).

In case of ZnO NPs from SD-CME and LD-CME, there was no inhibition of bacterial growth against any of the six pathogens (Figure 10: B&C).

Also there is no inhibition shown by ZnO NPs formed from callus treated under pH 5.0, pH 6.5, pH 7.0) on any of these six pathogens.

The present research work was an attempt to develop ZnO NPs with strong antibacterial potency by treating the callus from *C. roseus* under controlled light conditions and optimum pH to give nanoparticles with regulated attributes. This callus based route also maintains the sample availability throughout the year and medicinally prominent species can be used.

Alterations in light and pH vastly affect the growth and development of callus which is observed in the study via 2 different experiments. The callus was exposed to various light conditions: Controlled, SD, LD and observed for 7 & 14 days respectively for each photoperiod at pH 5.7. Induction and growth of callus

was found to be greatest at Controlled condition. In case of SD and LD, growth of callus gave a negative trend.

In another experiment, callus was treated in media with different pH 5.0, 6.5 and 7.0. But the results were the best at pH 5.7 in terms of development and pigmentation of callus. Distorted morphology and slow growth of callus were found at other pH.

Thus, ZnO NPs formed from CME-7 & 14 days (control light) and at pH 5.7 demonstrated greatest antibacterial action (in synergy with streptomycin) against all six pathogens at 1500 µg/ml concentration. For SD and LD conditions for both 7 & 14 days duration, there was no antibacterial activity observed. Also antibacterial activity was nil in case of ZnO NPs treated under different pH 5.0, 6.5 and 7.0.

The size of nanoparticles was confirmed by TEM analysis which revealed the average size as 50 nm. Hexagonal wurtzite shape in ZnO NPs was obtained only under controlled conditions. The FTIR confirmed the availability of different functional groups present within the phytochemicals constituent of callus extract. The XRD patterns showed the purity, phase composition of the synthesized nanoparticles. The EDX results obtained confirmed the metal composition in ZnO NPs. DLS confirmed uniform size distribution (dispersity index) while AFM revealed morphology.

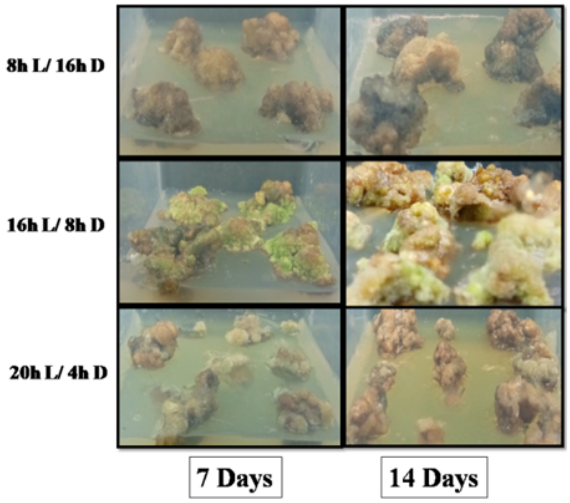

Light exposure (Hrs)		Explants	Observation
Light	Dark		
8 (Short Days)	16	Leaf	Black callus formation
16 (Control)	8	Leaf	Green callus formation
20 (Long Days)	4	Leaf	Yellow callus formation

Figure 1: Morphology of callus under different photoperiods and culture stages..

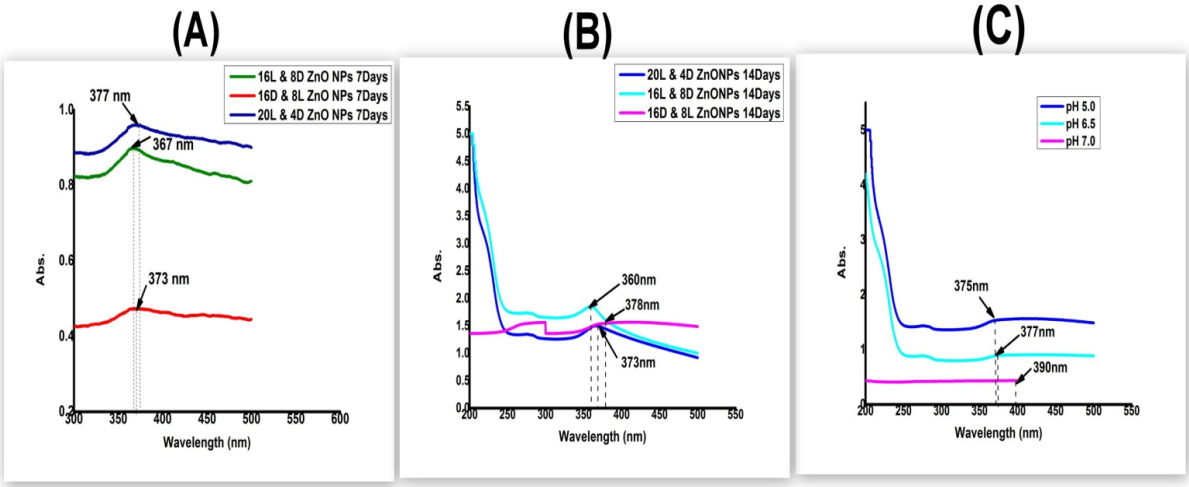

Figure 2: UV-visible spectra (A) 7 Days (B) 14 Days (C) Different pH.

 © 2021 Society of Education, India

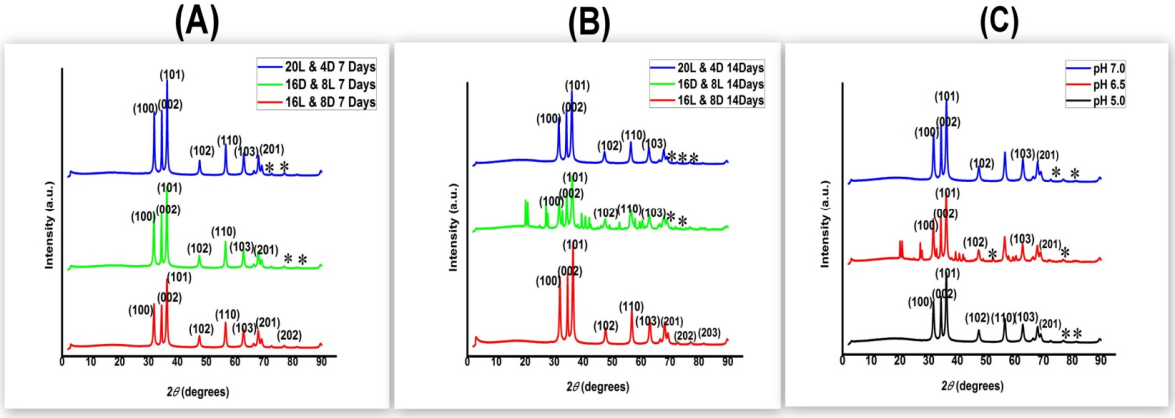

Fi

gure 3: XRD (A) 7 Days (B) 14 Days (C) Different pH.

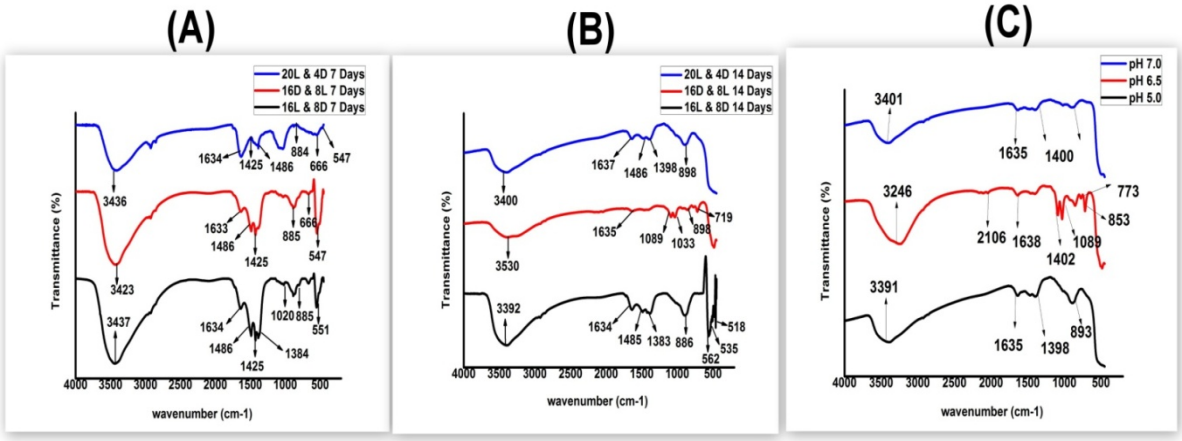

Figure 4: FTIR (A) 7 Days (B) 14 Days (C) Different pH.

Figure 5: EDX analysis (A1-A3) 7 Days (B1-B3) 14 Days (C1-C3) Different pH.

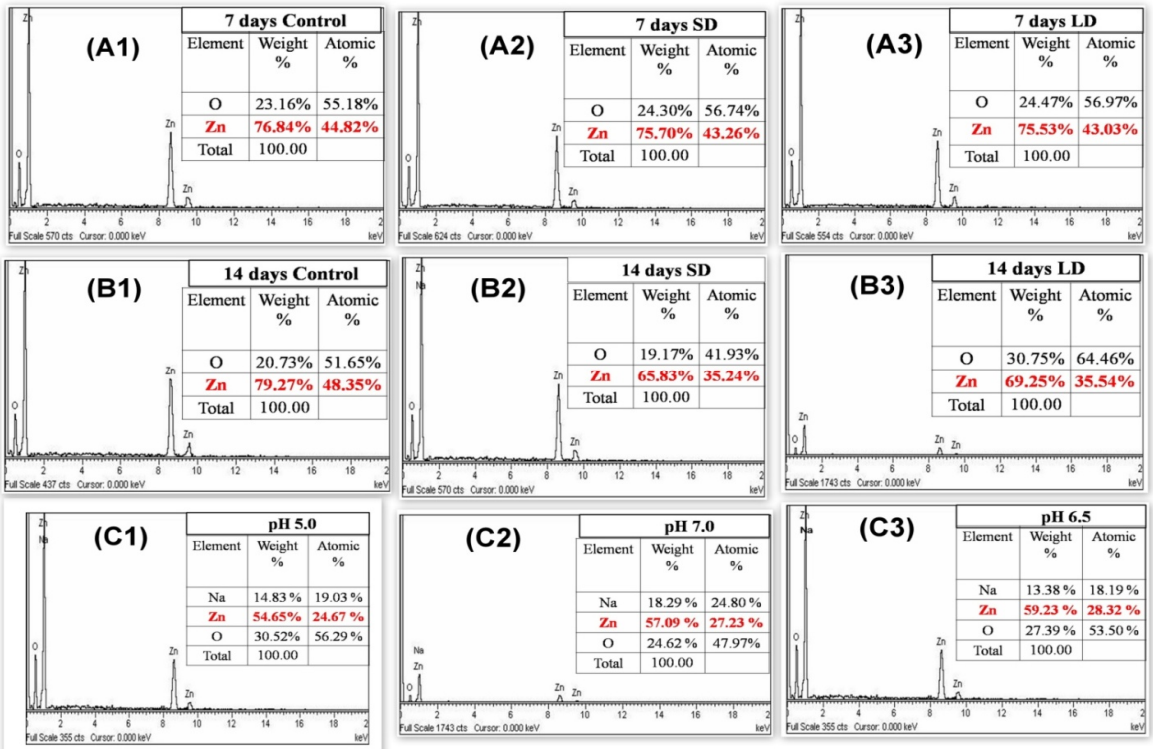

 © 2021 Society of Education, India

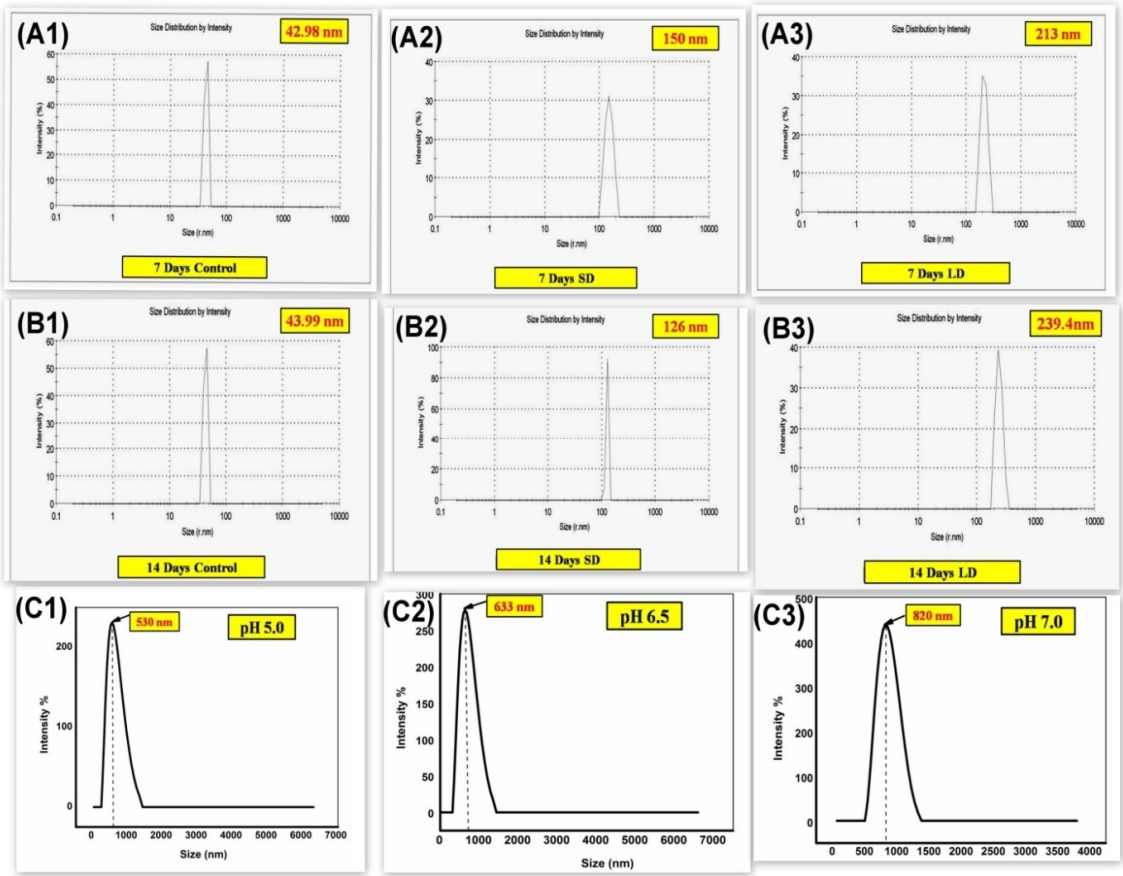

Figure 6: Particle size distribution (A1-A3) 7 Days (B1-B3) 14 Days (C1-C3) Different pH.

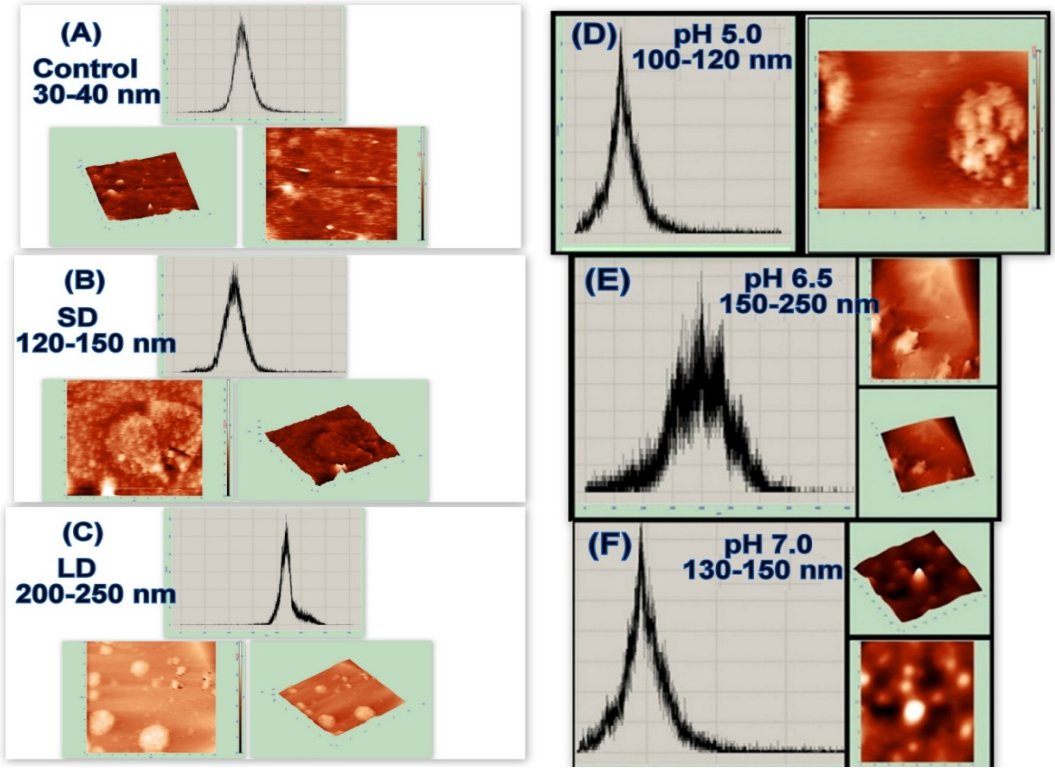

Figure 7: AFM images (A) 7 Days Control (B) 7 Days SD (C) 7 Days LD (D-F) Different pH.

 © 2021 Society of Education, India

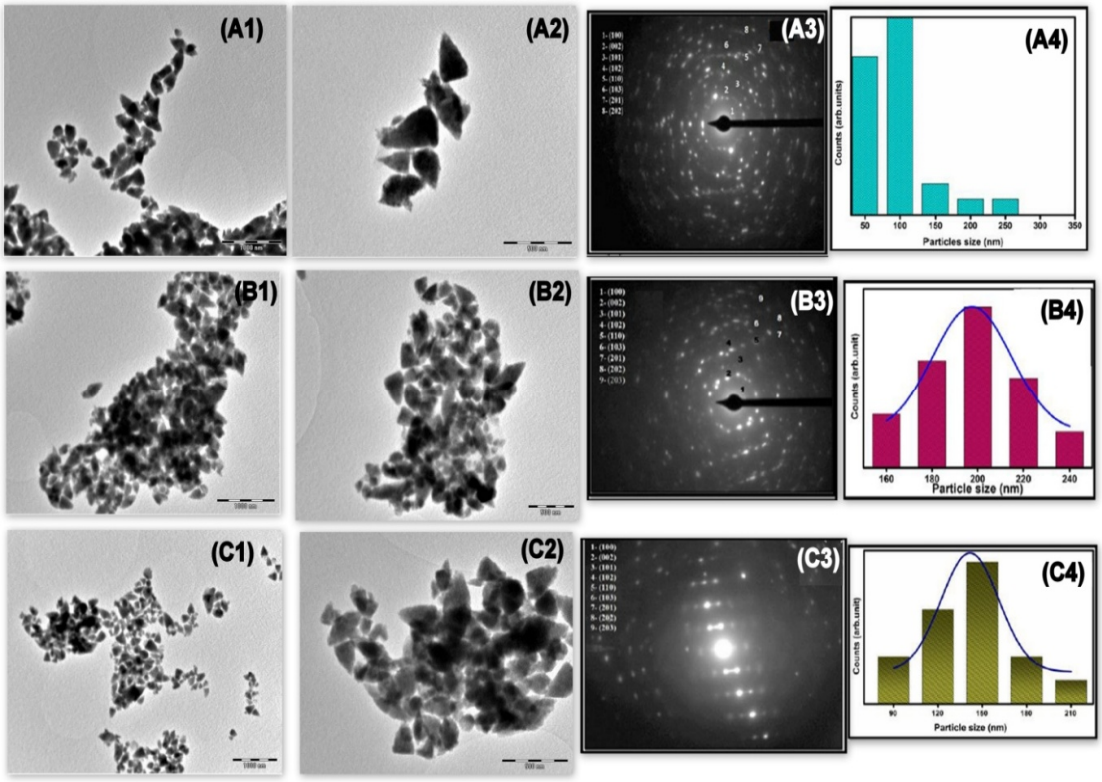

Figure 8: (A1-A4) 7 Days Control (B1-B4) 7 Days SD (C1-C4) 7 Days LD

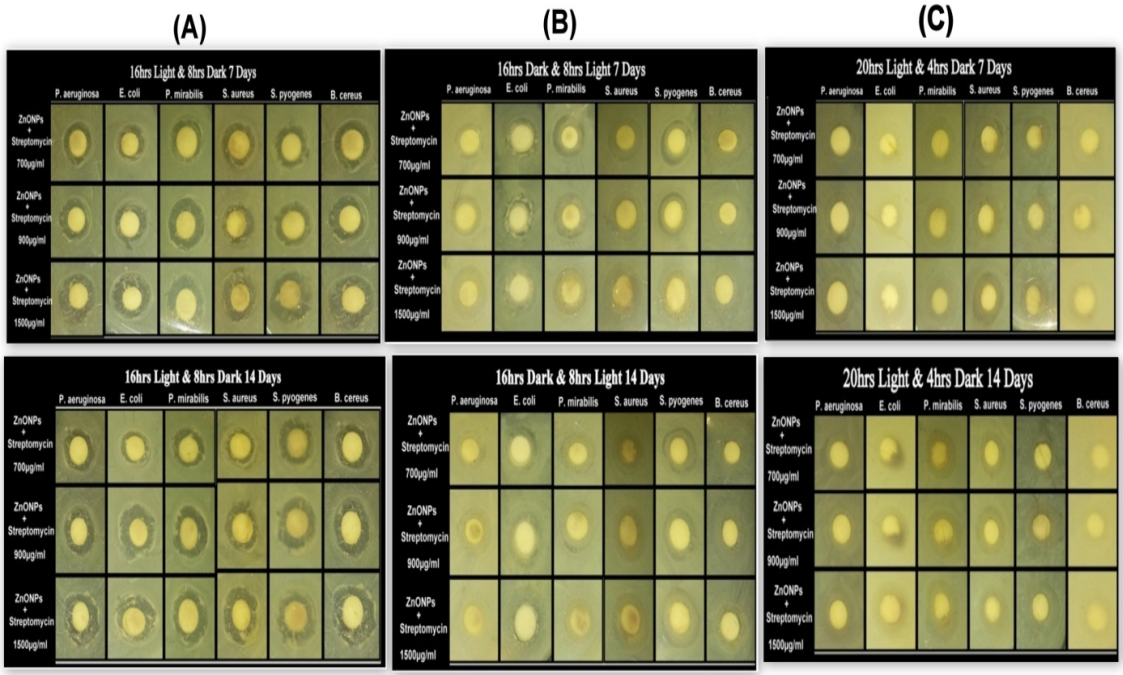

Figure 9: Antibacterial activity of 7 & 14 Days treated (A) Control, (B) SD (C) LD of ZnO NPs (700,900 and 1500µg/ml) and compared to ZnO NPs combined with antibiotic- streptomycin (10µg/ml) by ZOI measurement.

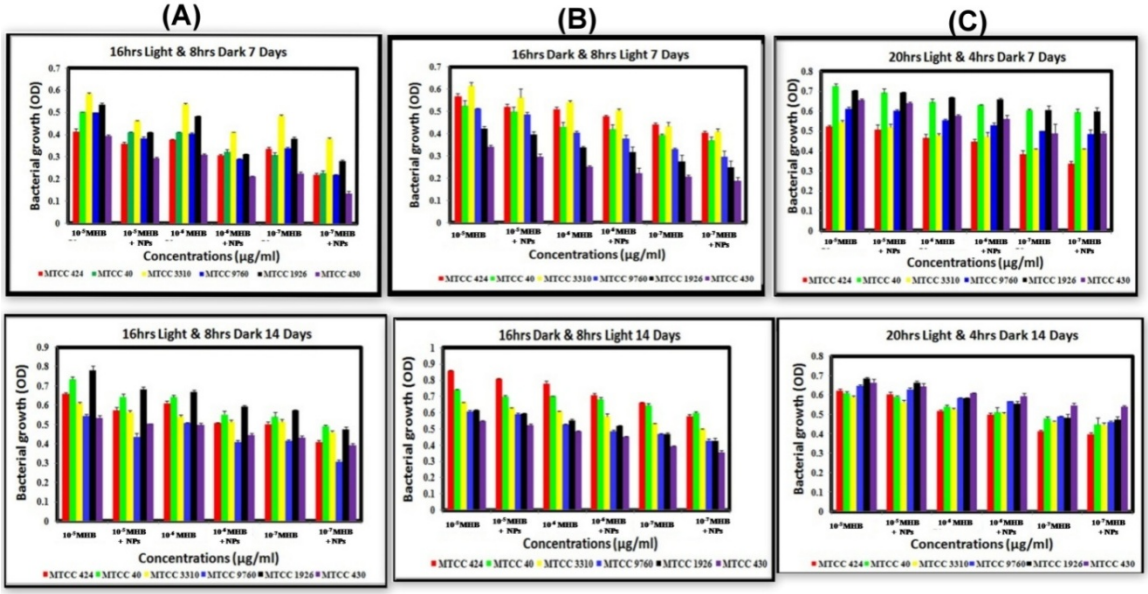

Figure 10: 7 & 14 Days treated (16hrs Light and 8hrs Dark, 16hrs Dark & 8hrs Light and 20hrs Light & 4hrs Dark) zinc oxide nanoparticles 1500µg/ml against microbes (Gram positive & Gram negative). Results are expressed as Mean±S.E.

Table 1.: Antibacterial activity of ZnO NPs and synergistic activity with streptomycin against pathogenic bacteria (Data shown in zone of inhibition (in mm)).

16hrs Light & 8hrs Dark 7 Days					
Bacteria	**Streptomycin (10µg/ml)**	**Single concentration of ZnONPs 900µg/ml**	**ZnONPs 700µg/ml + Streptomycin**	**ZnONPs 900µg/ml + Streptomycin**	**ZnONPs 1500µg/ml + Streptomycin**
***P. aeruginosa* MTCC 424**	11.03 ± 0.03	12.09 ± 0.01	13.33± 0.04	13.11 ± 0.11	15. 74 ± 0.83
***E. coli* MTCC 40**	10.40 ± 1.04	12.15 ± 0.03	13.58± 0.28	13.40 ± 0.74	14. 20 ± 0.39
***P. mirabilis* MTCC 3310**	11.09 ± 0.90	12.18 ± 0.03	15. 80 ± 0.19	13. 94 ± 0.03	16. 98 ± 0.51
***S. aureus* MTCC 9760**	11.06 ± 0.00	12. 30 ± 0.03	13.15 ± 0.06	14.60 ± 0.02	16. 01 ± 0.48
***S. pyogenes* MTCC 1926**	11.10 ± 0.01	12..35 ±0.02	15.18± 0.01	14. 12 ± 0.03	15. 98 ± 0.03
***B. cereus* MTCC 430**	11.12 ± 0.00	13. 01±0.00	13. 20± 0.01	14.37 ± 0.19	20.78 ± 0.15

16hrs Light & 8hrs Dark 14 Days					
Bacteria	**Streptomycin (10µg/ml)**	**Single concentration of ZnONPs 900µg/ml**	**ZnONPs 700µg/ml + Streptomycin**	**ZnONPs 900µg/ml + Streptomycin**	**ZnONPs 1500µg/ml + Streptomycin**
***P. aeruginosa* MTCC 424**	11.05 ± 0.03	12.15 ± 0.01	13.40± 0.04	14.00 ± 0.11	15. 98 ± 0.83
***E. coli* MTCC 40**	10.40 ± 1.04	12.20 ± 0.03	13.60± 0.28	13.98 ± 0.74	15. 20 ± 0.39
***P. mirabilis* MTCC 3310**	11.09 ± 0.90	12.78 ± 0.03	16. 01 ± 0.19	16. 94 ± 0.03	17. 08 ± 0.51
***S. aureus* MTCC 9760**	11.06 ± 0.00	12. 30 ± 0.03	13.45 ± 0.06	14. 98 ± 0.02	16. 98 ± 0.48
***S. pyogenes* MTCC 1926**	11.10 ± 0.01	12.40 ±0.02	15.78± 0.01	15. 98± 0.03	16. 08 ± 0.03
***B. cereus* MTCC 430**	11.12 ± 0.00	13. 10 ±0.00	13. 72± 0.01	14. 98 ± 0.19	21.78 ± 0.15

 © 2021 Society of Education, India

Table 2(A): Antibacterial activity of synthesized ZnO NPs and synergistic activity streptomycin against pathogenic bacteria (Data shown in zone of inhibition in mm.

16hrs Dark& 8hrs Light 7 Days					
Bacteria	**Streptomycin (10µg/ml)**	**Single concentration of ZnONPs 900µg/ml**	**ZnONPs 700µg/ml + Streptomycin**	**ZnONPs 900µg/ml + Streptomycin**	**ZnONPs 1500µg/ml + Streptomycin**
***P. aeruginosa* MTCC 424**	11.05 ± 0.03	11.06 ± 0.01	11.08 ± 0.01	11.09 ± 0.01	11.12 ± 0.04
***E. coli* MTCC 40**	10.40 ± 1.04	0.15 ± 0.02	0.58 ± 0.09	0.77 ± 0.04	0.95 ± 0.05
***P. mirabilis* MTCC 3310**	11.09 ± 0.90	0.19 ± 0.07	0.33 ± 0.05	0.61 ± 0.03	0.58 ± 0.43
***S. aureus* MTCC 9760**	11.06 ± 0.00	11.09 ± 2.17	11.09 ± 2.17	11.11 ± 0.01	11.14 ± 0.02
***S. pyogenes* MTCC 1926**	11.10 ± 0.01	11.10 ± 0.00	11.10 ± 0.00	11.10 ± 0.00	11.12 ± 0.04
***B. cereus* MTCC 430**	11.12 ± 0.00	0.78 ± 0.12	0.1 ± 0.01	0.07 ± 0.05	0.94 ± 0.06

16hrs Dark& 8hrs Light 14 Days					
Bacteria	**Streptomycin (10µg/ml)**	**Single concentration of ZnONPs 900µg/ml**	**ZnONPs 700µg/ml + Streptomycin**	**ZnONPs 900µg/ml + Streptomycin**	**ZnONPs 1500µg/ml + Streptomycin**
***P. aeruginosa* MTCC 424**	11.05 ± 0.03	11.06 ± 0.01	11.09± 0.04	11.09 ± 0.11	11. 11 ± 0.03
***E. coli* MTCC 40**	10.40 ± 1.04	0.15 ± 0.03	0.08 ± 0.08	0.04 ± 0.74	0.08 ± 0.39
***P. mirabilis* MTCC 3310**	11.09 ± 0.20	0.19 ± 0.02	0.02 ± 0.19	0.04 ± 0.03	0.15 ± 0.01
***S. aureus* MTCC 9760**	11.06 ± 0.00	11.10 ± 0.03	11.12 ± 0.06	11. 13 ± 0.01	11. 13 ± 0.48
***S. pyogenes* MTCC 1926**	11.10 ± 0.01	11.10 ±0.02	11.11± 0.01	11. 13± 0.05	11. 14 ± 0.03
***B. cereus* MTCC 430**	11.12 ± 0.00	0.38 ±0.00	0.2 ± 0.01	0. 09 ± 0.05	0.37 ± 0.10

Table 2(B): Antibacterial activity of synthesized ZnO NPs and synergistic activity streptomycin against pathogenic bacteria (Data shown in zone of inhibition in mm.

20hrs Light & 4hrs Dark 7 Days					
Bacteria	**Streptomycin (10µg/ml)**	**Single concentration of ZnONPs 900µg/ml**	**ZnONPs 700µg/ml + Streptomycin**	**ZnONPs 900µg/ml + Streptomycin**	**ZnONPs 1500µg/ml + Streptomycin**
***P. aeruginosa* MTCC 424**	11.05 ± 0.03	0.01 ± 0.01	0.03 ± 0.04	0.2 ± 0.17	0.03 ± 0.02
***E. coli* MTCC 40**	10.40 ± 1.04	0.02 ± 0.00	0.07 ± 0.01	0.03 ± 0.03	0.15 ± 0.21
***P. mirabilis* MTCC 3310**	11.09 ± 0.20	0.01 ± 0.00	0.02 ± 0.01	0.02 ± 0.03	0.00 ± 0.00
***S. aureus* MTCC 9760**	11.06 ± 0.00	0.03 ± 0.04	0.02 ± 0.00	0.03 ± 0.03	0.03 ± 0.04
***S. pyogenes* MTCC 1926**	11.10 ± 0.01	0.02 ± 0.01	0.03 ± 0.00	0.03 ± 0.02	0.04 ± 0.04
***B. cereus* MTCC 430**	11.12 ± 0.00	0.01 ± 0.00	0.04 ± 0.00	0.20 ± 0.25	0.10 ± 0.08

20hrs Light & 4hrs Dark 14 Days					
Bacteria	**Streptomycin (10µg/ml)**	**Single concentration of ZnONPs 900µg/ml**	**ZnONPs 700µg/ml + Streptomycin**	**ZnONPs 900µg/ml + Streptomycin**	**ZnONPs 1500µg/ml + Streptomycin**
***P. aeruginosa* MTCC 424**	11.05 ± 0.03	0.00 ± 0.01	0.11 ± 0.04	0.20 ± 0.17	0.07 ± 0.02
***E. coli* MTCC 40**	10.40 ± 1.04	0.02 ± 0.00	0.23± 0.01	0.27 ± 0.03	0.62 ± 0.21
***P. mirabilis* MTCC 3310**	11.09 ± 0.20	0.01 ± 0.00	0.03 ± 0.01	0.45 ± 0.03	0.04 ± 0.00
***S. aureus* MTCC 9760**	11.06 ± 0.00	0.03 ± 0.04	0.12 ± 0.00	0.03 ± 0.03	0.29 ± 0.04
***S. pyogenes* MTCC 1926**	11.10 ± 0.01	0.02 ± 0.01	0.23 ± 0.00	0.03 ± 0.02	0.61 ± 0.04
***B. cereus* MTCC 430**	11.12 ± 0.00	0.01 ± 0.00	0.14 ± 0.00	0.20 ± 0.25	0.37 ± 0.08

Table 3.: Antibacterial activity of ZnONPs and synergistic activity with streptomycin against pathogenic bacteria (Data shown in zone of inhibition in mm)

pH 5.0					
Bacteria	**Streptomycin (10µg/ml)**	**Single concentration of ZnONPs 900µg/ml**	**ZnONPs 700µg/ml + Streptomycin**	**ZnONPs 900µg/ml + Streptomycin**	**ZnONPs 1500µg/ml + Streptomycin**
***P. aeruginosa* MTCC 424**	11.33 ± 0.47	0.00 ± 0.00	0.01 ± 0.02	0.2 ± 0.01	0.02 ± 0.02
***E. coli* MTCC 40**	10.07 ± 0.94	0.03 ± 0.00	0.07 ± 0.01	0.03 ± 0.03	0.12 ± 0.15
***P. mirabilis* MTCC 3310**	11.33 ± 1.05	0.01 ± 0.00	0.03 ± 0.00	0.02 ± 0.03	0.00 ± 0.00
***S. aureus* MTCC 9760**	12.03 ± 0.07	0.04 ± 0.03	0.04 ± 0.05	0.03 ± 0.03	0.03 ± 0.04
***S. pyogenes* MTCC 1926**	12.36 ± 0.45	0.02 ± 0.01	0.03 ± 0.00	0.03 ± 0.02	0.05 ± 0.02
***B. cereus* MTCC 430**	12.46 ± 0.50	0.01 ± 0.00	0.04 ± 0.00	0.20 ± 0.25	0.10 ± 0.08

pH 6.5					
Bacteria	**Streptomycin (10µg/ml)**	**Single concentration of ZnONPs 900µg/ml**	**ZnONPs 700µg/ml + Streptomycin**	**ZnONPs 900µg/ml + Streptomycin**	**ZnONPs 1500µg/ml + Streptomycin**
***P. aeruginosa* MTCC 424**	11.33 ± 0.47	0.00 ± 0.00	0.2 ± 0.01	0.02 ± 0.02	0.02 ± 0.02
***E. coli* MTCC 40**	10.07 ± 0.94	0.03 ± 0.00	0.03 ± 0.03	0.12 ± 0.15	0.12 ± 0.15
***P. mirabilis* MTCC 3310**	11.33 ± 1.05	0.01 ± 0.00	0.02 ± 0.03	0.00 ± 0.00	0.00 ± 0.00
***S. aureus* MTCC 9760**	12.03 ± 0.07	0.04 ± 0.03	0.03 ± 0.03	0.03 ± 0.04	0.03 ± 0.04
***S. pyogenes* MTCC 1926**	12.36 ± 0.45	0.02 ± 0.01	0.03 ± 0.02	0.05 ± 0.02	0.05 ± 0.02
***B. cereus* MTCC 430**	12.46 ± 0.50	0.01 ± 0.00	0.20 ± 0.25	0.10 ± 0.08	0.10 ± 0.08

pH 7.0					
Bacteria	**Streptomycin (10µg/ml)**	**Single concentration of ZnONPs 900µg/ml**	**ZnONPs 700µg/ml + Streptomycin**	**ZnONPs 900µg/ml + Streptomycin**	**ZnONPs 1500µg/ml + Streptomycin**
***P. aeruginosa* MTCC 424**	11.33 ± 0.47	0.00 ± 0.00	0.01 ± 0.02	0.2 ± 0.01	0.02 ± 0.02
***E. coli* MTCC 40**	10.07 ± 0.94	0.03 ± 0.00	0.07 ± 0.01	0.03 ± 0.03	0.12 ± 0.15
***P. mirabilis* MTCC 3310**	11.33 ± 1.05	0.01 ± 0.00	0.03 ± 0.00	0.02 ± 0.03	0.00 ± 0.00
***S. aureus* MTCC 9760**	12.03 ± 0.07	0.04 ± 0.03	0.04 ± 0.05	0.03 ± 0.03	0.03 ± 0.04
***S. pyogenes* MTCC 1926**	12.36 ± 0.45	0.02 ± 0.01	0.03 ± 0.00	0.03 ± 0.02	0.05 ± 0.02
***B. cereus* MTCC 430**	12.46 ± 0.50	0.01 ± 0.00	0.04 ± 0.00	0.20 ± 0.25	0.10 ± 0.08

CONCLUSION

In conclusion the study offers the potential method to synthesize new economically viable potential green particles having high efficacy, less cytotoxic, feasibility, and eco friendly in nature. The antibacterial activity of nanoparticles individually and in combination with existing antibiotics and natural products will encourage checking more new compounds and also providing a new route against multi drug resistant bacteria. The synergistic effect also increase the efficiency of natural compounds at very low concentration that will help to treat more and more patients effectively. The green particles may decrease the dependency on synthetic drugs and also protect patient from the painful traditional methods of treatment.

FUTURE PROSPECTS

The ecofriendly synthesis of nanoparticles using callus extracts will prove as novel substrate for the large scale production. Synthesis of metal nanoparticles under controlled conditions by callus route will provide the opportunity for the regulation of shape and size of NPs which shall have multi-faceted applications of these nanoparticles.

The callus mediated nanoparticles have the potential to be used in various fields such as pharmaceuticals, therapeutics, drug delivery, food packaging industry and other commercial products as cosmetics, plastics, catalysts, nano-electronics etc. Presence of secondary metabolites and antioxidants further extends their role in agriculture. Green-synthesized ZnO NPs may be further explored as potential antimicrobial agent for wide spectrum of other infectious microorganisms. With the help of synergistic effect, dependency of synthetic drugs will be reduced and patients can thus be treated more effectively and saved from painful traditional methods of treatment. The combination of ZnO NPs with antibiotics will provide a novel path to develop new compounds to win battle against multi-drug resistant pathogens.

AUTHOR CONTRIBUTION

MG performed all the experiments and wrote the manuscript draft and design the concept and finalized the manuscript.

CONFLICT OF INTERESTS

The authors confirm they have no conflict of interests.

DATA AVAILABILITY STATEMENT IN YOUR MANUSCRIPT

All the raw data available

FUNDING STATEMENT

No funding available. AUMP Gwalior provided the money for research work.

ACKNOWLEDGEMENT

We wish to express our sincere acknowledgement to Dr. Ashok Kumar Chauhan, President, RBEF parent organization of Amity University Madhya Pradesh (AUMP), Dr. Aseem Chauhan, Additional President, RBEF and chairman of Amity University Gwalior Campus, Lt. Gen. V.K. Sharma, AVSM (Retd.), Vice

Chancellor of AUMP Gwalior Campus, for providing necessary facilities, their valuable support and encouragement throughout the work.

ABBREVIATIONS

AFM	Atomic force microscopy
ZnO NPs	Zinc oxide nanoparticles
BAP	Benzylaminopurine
CME	Callus mediate extract
DLS	Dynamic light scattering
EDX	Energy-dispersive X-ray
FTIR	Fourier Transform Infra Red spectroscopy
MHA	Muller hinton agar
MHB	Muller hinton broth
MS	Murashige and Skoog media
MIC	Minimum inhibitory concentration
NAA	Naphthalene acetic acid
PGRs	Plant growth regulators
SAED	Surface Area Electron Diffraction
SPR	Surface Plasmon Resonance
TEM	Transmission Electron Microscopy
XRD	X Ray Diffraction spectroscopy
ZOI	Zone of inhibition
16h Light/8h Dark	Control Condition
16h Dark /8h Light (SD)	Short Days Condition
20h Light/4h Dark (LD)	Long Days Condition

REFERENCES

1. Purkait, P. K., Roy, J., Maitra, S., and Choudhuri, M. G. (2015). Green Synthesis of Zinc Oxide Nanoparticles – A Review, science voyage, 1(2), 32-46.
2. Rao, P., Kota, S. K., Manja, S.(2007). Biosynthesis of Zinc Nanoparticles and their Applications. International Journal of Research and Scientific Innovation (IJRSI).
3. Jiang, J., Pi, J., & Cai, J. (2018). The advancing of zinc oxide nanoparticles for biomedical applications. Bioinorganic chemistry and applications, 2018.
4. Naveed Ul Haq, A., Nadhman, A., Ullah, I., Mustafa, G., Yasinzai, M., & Khan, I. (2017). Synthesis approaches of zinc oxide nanoparticles: the dilemma of ecotoxicity. Journal of Nanomaterials, 2017.
5. Thongam, D. D., Gupta, J., Sahu, N. K., & Bahadur, D. (2018). Investigating the role of different reducing agents, molar ratios, and synthesis medium over the formation of ZnO nanostructures and their photo-catalytic activity. Journal of materials science, 53(2), 1110-1122.
6. Jin, S. E., Jin, J. E., Hwang, W., & Hong, S. W. (2019). Photocatalytic antibacterial application of zinc oxide nanoparticles and self-assembled networks under dual UV irradiation for enhanced disinfection. International journal of nanomedicine, 14, 1737.
7. Da Silva, J. A. T., Winarto, B., Dobránszki, J., & Zeng, S. (2015). Disinfection procedures for in vitro propagation of Anthurium. Folia Horticulturae, 27(1), 3-14.
8. Thomas, T. D., & Shankar, S. (2009). Multiple shoot induction and callus regeneration in Sarcostemma brevistigma Wight & Arnott, a rare medicinal plant. Plant Biotechnology Reports, 3(1), 67.
9. Prakash, M. B., & Paul, S. (2012). Green synthesis of silver nanoparticles using Vinca roseus leaf extract and evaluation of their antimicrobial activities. Int J Appl Biol Pharma Technol 3(4),105–111.
10. Gnanasangeetha, D., & Thambavani, D. S. (2013). Biogenic production of zinc oxide nanoparticles using Acalypha indica. Journal of Chemical, Biological and Physical Sciences (JCBPS), 4(1), 238.
11. Jamdagni, P., Khatri, P., & Rana, J. S. (2018). Green synthesis of zinc oxide nanoparticles using flower extract of Nyctanthes arbor-tristis and their antifungal activity. Journal of King Saud University-Science, 30(2), 168-175.
12. Gupta M, Tomar R S, Mishra R K. Factors affecting biosynthesis of green nanoparticles". *Our Heritage*, 2020.
13. Rakholiya, K., & Chanda, S. (2012). In vitro interaction of certain antimicrobial agents in combination with plant extracts against some pathogenic bacterial strains. Asian Pacific Journal of Tropical Biomedicine, 2(3), S1466-S1470.
14. Diao, W. R., Hu, Q. P., Feng, S. S., Li, W. Q., & Xu, J. G. (2013). Chemical composition and antibacterial activity of the essential oil from green huajiao (Zanthoxylum schinifolium) against selected food borne pathogens. Journal of agricultural and food chemistry, 61(25), 6044-6049.
15. Dobrucka, R., & Długaszewska, J. (2016). Biosynthesis and antibacterial activity of ZnO nanoparticles using Trifolium pratense flower extract. Saudi journal of biological sciences, 23(4), 517-523.

16. Kami, C., Lorrain, S., Hornitschek, P., & Fankhauser, C. (2010). Light-regulated plant growth and development. In Current topics in developmental biology 91, 29-66. Academic Press.
17. Gupta M, Tomar R S, Kaushik S, Sharma D, Mishra R K. (2018). Effective antimicrobial activity of green ZnO nano particles of *Catharanthus roseus*. Frontiers in Microbiology.123-129
18. Vennila, S., & Jesurani, S. S. (2017). Eco-friendly green synthesis and characterization of stable ZnO Nanoparticle using small Gooseberry fruits extracts. International Journal of Chem Tech Research, 10(5).
19. Aromal, S. A., & Philip, D. (2012). Green synthesis of gold nanoparticles using Trigonella foenum-graecum and its size-dependent catalytic activity. Spectrochimica Acta Part A: Molecular and Biomolecular Spectroscopy, 97, 1-5.
20. Marquis, R. E., Mayzel, K., & Carstensen, E. L. (1976). Cation exchange in cell walls of gram-positive bacteria. Canadian journal of microbiology, 22(7), 975-982.
21. Raghupathi, K. R., Koodali, R. T., & Manna, A. C. (2011). Size-dependent bacterial growth inhibition and mechanism of antibacterial activity of zinc oxide nanoparticles. Langmuir, 27(7), 4020-4028.

Copyright: © 2021 Society of Education. This is an open access article distributed under the Creative Commons Attribution License, which permits unrestricted use, distribution, and reproduction in any medium, provided the original work is properly cited.